

Systematic Interactome Mapping and Genetic Perturbation Analysis of a *C. elegans* TGF- β Signaling Network

Muneesh Tewari,^{1,2,3,4,12} Patrick J. Hu,^{4,5,6,12}
Jin Sook Ahn,^{1,2,4} Nono Ayivi-Guedeoussou,^{1,2,4}
Pierre-Olivier Vidalain,^{1,2,4} Siming Li,^{1,2,4}
Stuart Milstein,^{1,2,4} Chris M. Armstrong,^{1,2,4}
Mike Boxem,^{1,2,4} Maurice D. Butler,^{2,4,5}
Svetlana Busiguina,^{2,7} Jean-François Rual,^{1,2,4,8}
Nieves Ibarrola,⁹ Sabrina T. Chaklos,^{2,4,13}
Nicolas Bertin,^{1,2,4} Philippe Vaglio,^{2,4,14}
Mark L. Edgley,^{10,15} Kevin V. King,¹¹
Patrice S. Albert,¹⁰ Jean Vandenhaute,^{2,4,8}
Akhilesh Pandey,⁹ Donald L. Riddle,¹⁰
Gary Ruvkun,^{4,5} and Marc Vidal^{1,2,4,*}

¹Center for Cancer Systems Biology

²Department of Cancer Biology

³Department of Medical Oncology
Dana-Farber Cancer Institute

⁴Department of Genetics
Harvard Medical School

Boston, Massachusetts 02115

⁵Department of Molecular Biology

⁶Division of Hematology/Oncology
Massachusetts General Hospital
Boston, Massachusetts 02114

⁷Laboratory of Neuroendocrinology
Cajal Institute

Consejo Superior de Investigaciones Cientificas
28002 Madrid
Spain

⁸Unité de Recherche en Biologie Moléculaire
Facultés Notre-Dame de la Paix
Namur 5000
Belgium

⁹McKusick-Nathans Institute of Genetic Medicine
Johns Hopkins University
Baltimore, Maryland 21287

¹⁰Division of Biological Sciences and
Molecular Biology Program
University of Missouri

Columbia, Missouri 65211

¹¹Midwest Research Institute
Kansas City, Missouri 64110

Summary

To initiate a system-level analysis of *C. elegans* DAF-7/TGF- β signaling, we combined interactome mapping with single and double genetic perturbations. Yeast two-hybrid (Y2H) screens starting with known DAF-7/TGF- β pathway components defined a network of 71 interactions among 59 proteins. Coaffinity purification (co-AP) assays in mammalian cells confirmed the

overall quality of this network. Systematic perturbations of the network using RNAi, both in wild-type and *daf-7/TGF- β* pathway mutant animals, identified nine DAF-7/TGF- β signaling modifiers, seven of which are conserved in humans. We show that one of these has functional homology to human SNO/SKI oncoproteins and that mutations at the corresponding genetic locus *daf-5* confer defects in DAF-7/TGF- β signaling. Our results reveal substantial molecular complexity in DAF-7/TGF- β signal transduction. Integrating interactome maps with systematic genetic perturbations may be useful for developing a systems biology approach to this and other signaling modules.

Introduction

With the public release of (nearly) complete genome sequences, the availability of draft versions of the corresponding predicted proteomes, and the advent of functional genomic and proteomic approaches for large-scale identification and characterization of gene products, we are beginning to understand biological processes at the level of systems (Ideker et al., 2001; Kitano, 2002; Vidal, 2001). One step toward meeting this challenge has been the development of large-scale protein interaction (or “interactome”) mapping strategies (Walhout and Vidal, 2001b). In multicellular organisms, interactome maps have been used to identify components of various biological systems and draw networks of possible connections among them (Walhout et al., 2000a). Thus far, however, the use of interactome maps has been somewhat limited for systems biology approaches, because such maps lack information pertaining to the logic of molecular networks, which resides more in the functional relationships between components than in their physical interactions alone (Ge et al., 2003).

Experimental evidence for functional involvement of potential network components identified by high throughput yeast two-hybrid (HT-Y2H) screens can be obtained by RNAi knockdowns of the corresponding genes (Boulton et al., 2002; Walhout et al., 2002). However, to reveal functional interactions between network components, the consequences of simultaneous perturbations of two or more components must be examined. This kind of analysis is routine in classical genetics to identify functional relationships, such as epistatic and synthetic enhancement interactions between genes (Avery and Wasserman, 1992; Guarente, 1993). This is typically performed a few genes at a time. However, the combination of interactome mapping and systematic large-scale double perturbation genetic analysis has not been described to date. Here, we report such an analysis performed in the context of the *C. elegans* DAF-7/TGF- β signaling network.

Signaling through ligands of the TGF- β superfamily serves important functions in diverse species, including roles in cancer pathogenesis, inflammation, and development (Massague, 1998). Inherited mutations in genes encoding components of TGF- β signaling pathways

*Correspondence: marc_vidal@dfci.harvard.edu

¹²These authors contributed equally to this work.

¹³Present address: Tufts University School of Medicine, Boston, Massachusetts 02111.

¹⁴Present address: Modul-Bio, 13009 Marseille, France.

¹⁵Present address: Biotechnology Laboratory, University of British Columbia, Vancouver, BC V6T 1Z3, Canada.

cause a variety of diseases, including familial primary pulmonary hypertension, hereditary chondrodysplasia, and tumor predisposition syndromes (Massague et al., 2000). In *C. elegans*, the *daf-7/TGF- β* pathway regulates a decision between reproductive development and arrest at a larval stage known as dauer that is suited for survival under conditions of environmental stress (Riddle, 1988). Dauer larvae can be discriminated from other larval stages and adults based on radial constriction, the presence of alae, the absence of pharyngeal pumping, darkened intestinal appearance, and other morphological features. Components of the *daf-7/TGF- β* pathway have been identified and characterized genetically (Thomas et al., 1993) and are conserved with the canonical TGF- β signaling pathway in vertebrates (Estevez et al., 1993; Georgi et al., 1990; Inoue and Thomas, 2000; Patterson et al., 1997; Ren et al., 1996; Schackwitz et al., 1996) (Figure 1A). Loss-of-function mutations in upstream components (Figure 1A; see pink rectangles) produce an enhanced dauer arrest phenotype, whereas similar mutations in downstream components (Figure 1A; see green rectangles) produce an inability to undergo dauer arrest.

Large-scale Y2H screens using known DAF-7/TGF- β pathway components as initial baits produced an interactome network that we interrogated *in vivo* using single and double genetic perturbations performed with RNAi and genetic loss-of-function mutants. Here, we identify several modulators of DAF-7/TGF- β signaling and infer some of their functional relationships from patterns of genetic interaction.

Results and Discussion

Y2H Interactome Mapping of a DAF-7/TGF- β Network

We performed Y2H screens using a mixed-stage *C. elegans* cDNA library fused to the activation domain-encoding sequence of Gal4 (AD-wrmcDNA) (Walhout and Vidal, 2001a). We used as baits six of the known DAF-7/TGF- β pathway proteins fused to the Gal4 DNA binding domain (DB-X) (i.e. DAF-7, a TGF- β superfamily ligand [Ren et al., 1996]; DAF-1 [Georgi et al., 1990] and DAF-4 [Estevez et al., 1993], two heteromeric TGF- β receptor homologs; DAF-14, a SMAD2 homolog [Inoue and Thomas, 2000]; DAF-3, a SMAD4 homolog [Patterson et al., 1997]; and DAF-12, a nuclear hormone receptor [NHR] [Antebi et al., 2000] [Figure 1A]). An ORF corresponding to DAF-8, an R-SMAD homolog (Estevez, 1997), was cloned as a bait but could not be used in Y2H screens because the DB-DAF-8 fusion behaved as a strong autoactivator. One additional gene known to act in this pathway, *daf-5* (Figure 1A), was not used as a bait because it had not been molecularly cloned prior to the present work (see later results).

To minimize false positive interactions, we utilized a version of the two-hybrid system that expresses bait and prey proteins from low-copy vectors and a mild *ADH1* promoter (Vidal, 1997). We also retested all interactions by reconstituting them in fresh yeast cells containing the bait plasmid and retransformed with the prey plasmid by gap repair (Walhout and Vidal, 2001a). From screens using the initial six baits, we recovered 28 potentially interacting proteins (Figure 1B; see blue circles).

We expanded this interactome map with “second-generation” proteome-wide Y2H screens using 19 of the 28 Y2H interactors identified from the first-generation screens as baits (see Experimental Procedures for details). A total of 27 additional interactors were identified (Figure 1B; see yellow circles). Altogether, we identified 71 Y2H interactions among 59 proteins, comprising a complex interactome network (Figure 1B; Supplemental Table S1 at <http://www.molecule.org/cgi/content/full/13/4/469/DC1>).

Overall Validation of the DAF-7/TGF- β Y2H Interactome Network by Co-AP Assays in 293T Cells

To evaluate the accuracy of our HT-Y2H interactome data set, we considered experimental and biological false positives separately. Experimental false positives arise from inherent limitations specific to the Y2H method, while biological false positives correspond to X-Y protein pairs that can interact in various exogenous and artificial assays but do not do so *in vivo* in their natural “environment.”

To directly test the rate of experimental false positives in our Y2H screens, we retested interactions using an independent assay based on co-AP of bait and prey proteins expressed in transfected mammalian cells (Xu et al., 2003). ORFs cloned here or available in the ORFeome 1.1 collection (Reboul et al., 2003) were Gateway transferred into the relevant mammalian cell expression vectors (Walhout et al., 2000b). Bait proteins were expressed as glutathione S-transferase (GST) fusions (Smith and Johnson, 1988) and prey proteins as Myc epitope-tagged fusions in the human 293T cell line. GST fusion proteins were precipitated from cell lysates by glutathione-Sepharose affinity chromatography, and associated prey proteins were detected by immunoblotting precipitates with anti-Myc antibody.

Among 19 Y2H pairs for which both GST-bait and Myc-prey fusion proteins were adequately expressed (see Experimental Procedures for details), 17 interactions (89%) were recapitulated (Figure 2). This experiment strongly indicates that we have generated a high-quality DAF-7/TGF- β interactome network with a very low frequency of experimental false positive interactions.

It is important to note that until we have a precise and dynamic view of the whole proteome of an organism of interest, it will be virtually impossible to establish that any two proteins found by Y2H do *not* interact *in vivo*. Thus, biological false positives are much more difficult to define and detect. However, increasing evidence for biologically genuine Y2H interactions can be obtained by accumulating experimental evidence emerging from other functional genomic or proteomic approaches (Ge et al., 2003; Vidal, 2001).

Limitations of the Y2H-Generated Interactome Network

Although our Y2H screens identified 71 protein interactions, it is likely that there are additional interactome components that were not identified by this approach. Y2H screening has been estimated to have a false negative rate of approximately 60%–70% (Walhout et al.,

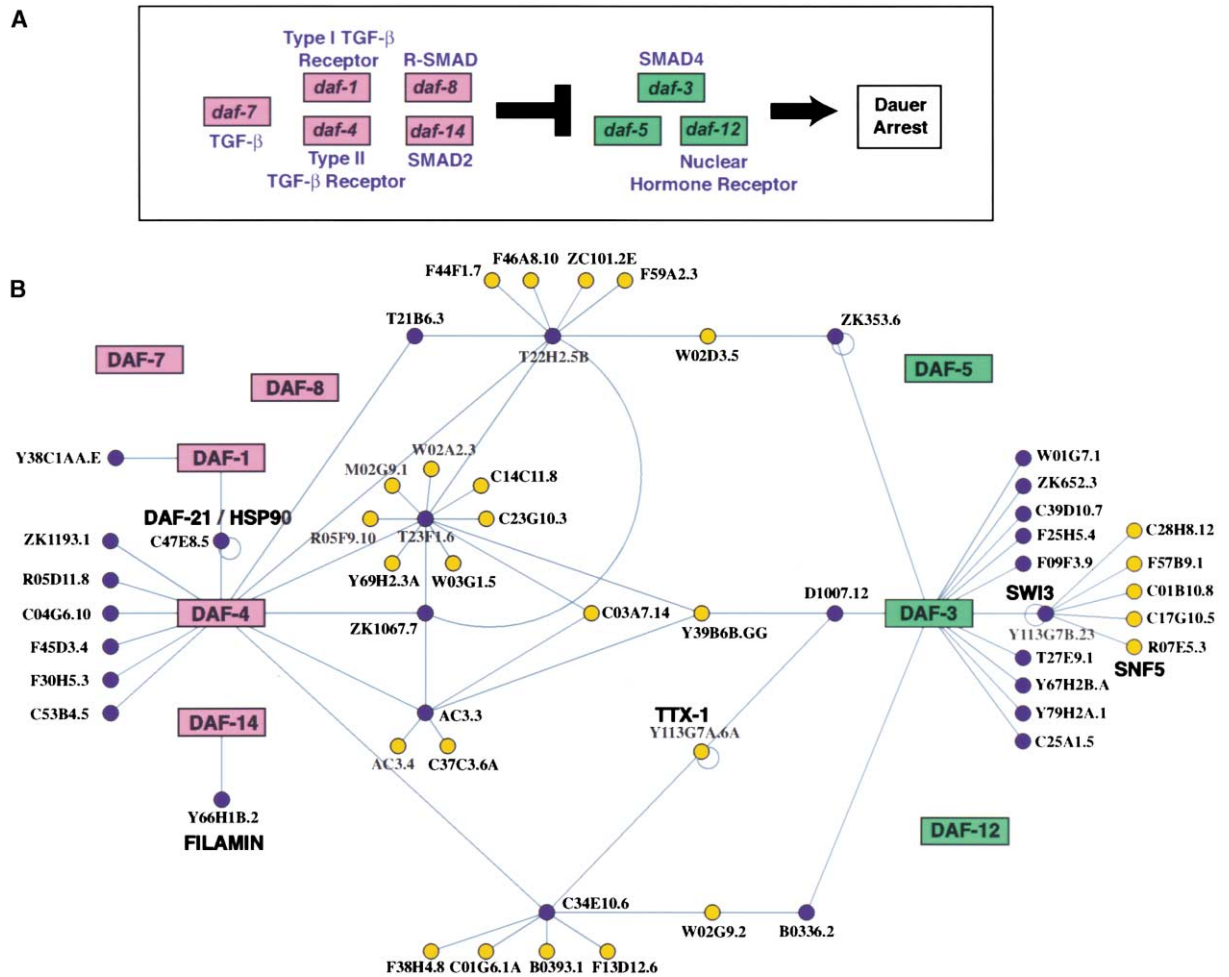


Figure 1. A *C. elegans* DAF-7/TGF- β Signaling Network

(A) Model of *daf-7*/TGF- β signaling as defined by genetic analysis. The activity of the pathway determines the decision between dauer arrest and development to a reproductive adult. Genes inferred to function to repress dauer formation in the wild-type state are indicated in pink, whereas those that act to induce dauer arrest in the wild-type state are indicated in green. As indicated by the black "stopped" arrow, the genes in green are epistatic to the genes in pink. *C. elegans* gene names are indicated in italics, with mammalian homologs of their encoded products indicated in blue. Molecular cloning of *daf-5* has not been previously published (see later results presented here). At the biochemical level, the pathway is believed to be initiated by binding of the TGF- β -like ligand DAF-7 to a heteromeric cell surface receptor (composed of DAF-1/TGF- β -receptor type I and DAF-4/TGF- β -receptor type II). According to the current model, DAF-8 (an R-SMAD) and DAF-14 (a SMAD2 homolog) become activated, leading to action on downstream components, which include the SMAD4 homolog DAF-3 and the nuclear hormone receptor DAF-12.

(B) A *C. elegans* DAF-7/TGF- β interactome network. Links represent Y2H interactions. Pink or green rectangles represent known *daf-7*/TGF- β signaling components. Screens done using DAF-7 and DAF-12 as baits did not yield any interactors. DAF-8/R-SMAD autoactivated Y2H reporter genes and could therefore not be used as a bait. DAF-5 was not used as an initial bait in Y2H screens because molecular cloning of *daf-5* had not been published until the present work (see later results). Blue circles represent first-generation interactors. Yellow circles represent second-generation interactors. WormPep-predicted ORF names are indicated for each of the interactors. Circular links represent homotypic protein interactions. Interactors already implicated in *daf-7*/TGF- β or dauer signaling on the basis of published studies are highlighted by providing alternative names in larger bold letters.

2000a). Interactions requiring specific phosphorylation states of the baits, for instance, might not be detected in this assay. Protein interactions among DAF-7/TGF- β components in *C. elegans* have not been studied in the past. However, if one infers expected protein interactions on the basis of known interactions in other species, it is apparent that most of the predicted interactions (many of which are phosphorylation dependent) were not found in our screens. The false negative rate might be particularly prominent in our experiments because of the rigorous constraints used to minimize the false

positive rate. Although our interactome network is not comprehensive, the co-AP experiments along with results of functional assays (see below) suggest that this approach has nonetheless identified many components of TGF- β signaling.

Proteins in the Interactome Network with Likely Links to DAF-7/TGF- β Signaling and/or Dauer Formation
Searches of the scientific literature provided immediate links to TGF- β signaling and/or dauer formation for some of the proteins in the interactome map. One component

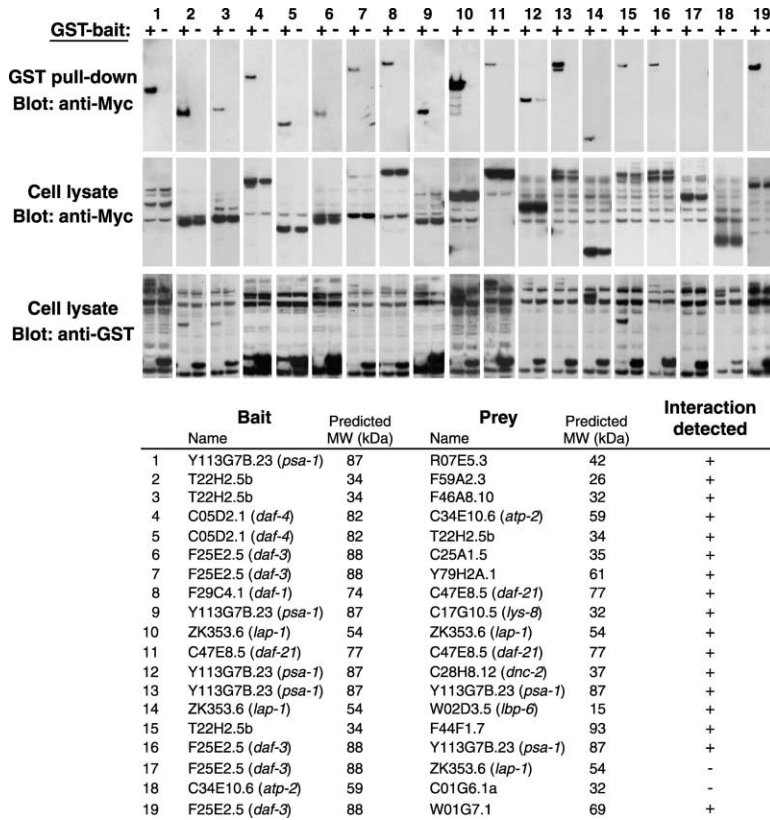


Figure 2. Recapitulation of Y2H Interactions in Mammalian Cells

Upper panels show the results of anti-Myc immunoblotting of glutathione-Sepharose precipitates from cells transfected with GST^{+/−}-bait and Myc-prey fusion protein expression vectors. The lanes alternate between extracts from cells expressing GST-bait proteins (+) or GST alone (−). Aliquots of cell lysates were also directly immunoblotted to detect expression of Myc- and GST-tagged proteins (middle and lower panels, respectively). Expression of GST protein was consistently observed at much higher levels than GST-bait proteins. Despite this, specific co-AP of Myc-prey protein is detected in GST-bait-transfected samples as compared to GST-transfected samples in 17 out of 19 cases. ORF names (and gene names in parentheses) corresponding to baits and preys are shown below the immunoblots. Approximate molecular weights of the protein predicted from each ORF do not include the contribution of GST- or of the Myc-epitope tag.

of the network, C47E8.5, is an Hsp90 protein that interacts with both DAF-1/TGF-β-RI and DAF-4/TGF-β-RII. C47E8.5 also corresponds to *daf-21* (Figure 1B), a gene previously implicated in dauer formation by virtue of a gain-of-function mutation that confers an enhanced dauer arrest phenotype (Birnbay et al., 2000). Genetic epistasis analysis places this gain-of-function allele in the *daf-11*/guanyl cyclase pathway (Thomas et al., 1993). *daf-11* encodes a guanyl cyclase that is expressed in a subset of amphid neurons, the processes of which are exposed to the environment (Birnbay et al., 2000). Although genetic analysis suggests that DAF-11/guanyl cyclase and the DAF-21/Hsp90 gain-of-function mutant protein signal in parallel to the *daf-7*/TGF-β pathway (Thomas et al., 1993), the interaction with both DAF-1/TGF-β-RI and DAF-4/TGF-β-RII (Figure 1B) suggests that wild-type DAF-21/Hsp90 may function in the DAF-7/TGF-β pathway.

The TTX-1 homeoprotein (Y113G7A.6A) is linked to both DAF-3/SMAD4 and DAF-4/TGF-β-RII through one interactor (Figure 1B). TTX-1 is encoded by a gene that is required for sustained dauer arrest in *daf-7*/TGF-β loss-of-function mutant animals (Satterlee et al., 2001). One explanation for this observation has been that *ttx-1* may affect dauer maintenance because of its role in specification of neurons that transduce the thermal inputs that are important in dauer regulation. Our results suggest an alternative model in which the TTX-1 protein may function more directly by interacting with DAF-7/TGF-β pathway signaling proteins to regulate maintenance of the dauer state. The protein interaction data

would predict that TTX-1 acts in the same cells as DAF-3/SMAD4 and DAF-4/TGF-β-RII.

Another protein in the network, Y66H1B.2, is a homolog of human filamin and interacts with DAF-14/SMAD2 (Figure 1B). This recapitulates the reported interaction between human filamin and SMAD2 in cultured mammalian cells (Sasaki et al., 2001). Filamin is known to function as a modulator of TGF-β signaling, since expression of filamin in filamin-deficient mammalian cells has been shown to restore TGF-β signaling (Sasaki et al., 2001).

Data from the interaction map also suggests hypotheses relevant to understanding the function of known DAF-7/TGF-β pathway components. For example, DAF-3/SMAD4 is known to act as a transcriptional repressor in cells of the *C. elegans* pharynx (Thatcher et al., 1999). In our Y2H screens, DAF-3/SMAD4 interacted with Y113G7B.23, which in turn interacted with R07E5.3. These two genes encode homologs of SWI3 and SNF5, respectively, which are chromatin-remodeling factors that can participate in transcriptional repression (Klochendler-Yeivin et al., 2002). Hence, it is possible that transcriptional repression by DAF-3/SMAD4 is at least in part mediated by these chromatin-associated factors.

An important aim of our study was to identify molecules relevant to human TGF-β signaling pathways. At least 29 of the 55 identified proteins in the interactome network (54%) appear to show strong sequence conservation in humans by BLASTP analysis, suggesting that many of these interactions may be relevant to mammalian TGF-β signaling (Supplemental Table S2, available on *Molecular Cell's* website).

Functional Analysis of Interactome Components by Systematic Genetic Perturbations

Given that the majority of the proteome has not been studied, a general limitation of protein interaction maps is that most interactors represent uncharacterized proteins. Without functional data on these proteins, the biological relevance of these interactions is often difficult to ascertain. Indeed, the majority of proteins in our interactome network do not have known biological functions.

RNAi can be performed in wild-type animals (i.e., single genetic perturbations) to assign functional roles to individual proteins in an interactome network (Boulton et al., 2002). We carried out single perturbation analysis of proteins from the interactome network using RNAi and assayed for an enhanced dauer arrest phenotype. Three genes derived from the protein interaction network produced an enhanced dauer arrest phenotype upon RNAi in wild-type animals (C25A1.5, T27E9.1, and B0336.2/*arf-1*; Figure 3A, wild-type row, and Figure 3B, blue rows), indicating that these gene products normally function to repress dauer formation during larval development.

Single perturbation analysis, although capable of directing attention to particular components in an interactome network, does not reveal functional relationships with directions or signs between components (e.g. X acts upstream of Y or X represses Y). An understanding of such functional relationships is essential for deciphering the logic of molecular networks. Simultaneous perturbation of multiple components is a strategy that may reveal such relationships. To identify functional relationships in the DAF-7/TGF- β interactome network, we carried out systematic double genetic perturbations by performing RNAi of identified interactome components in various loss-of-function mutant backgrounds corresponding to known DAF-7/TGF- β pathway components. These double perturbations identified 13 genetic interactions among genes encoding components of the DAF-7/TGF- β interactome. First, all three genes found to have an enhanced dauer arrest RNAi phenotype in wild-type animals (T27E9.1, B0336.2/*arf-1*, and C25A1.5) demonstrated a genetic interaction with the known *daf-7*/TGF- β pathway gene *daf-12*/NHR (Figures 3A and 3C). The nature of this interaction was epistatic, given that the *daf-12*(*m20*) loss-of-function allele suppressed the enhanced dauer arrest RNAi phenotype of each of the three genes (Figures 3A and 3C). This suggests that these three gene products normally function upstream of DAF-12/NHR to repress dauer formation.

A number of additional epistatic interactions were identified involving W01G7.1, a gene encoding an interactome component that physically interacts with DAF-3/SMAD4 (Figures 1B and 2, experiment 19). RNAi of W01G7.1 suppressed the enhanced dauer arrest phenotype of loss-of-function mutants in *daf-1*/TGF- β -RI, *daf-7*/TGF- β , *daf-8*/R-SMAD, and *daf-14*/SMAD2 (Figures 3A and 3B). This suggests that the W01G7.1 gene product may function downstream of and be repressed by DAF-1/TGF- β -R1, DAF-7/TGF- β , DAF-8/R-SMAD, and DAF-14/SMAD2.

In addition to epistatic interactions, synthetic enhancement was also observed. RNAi of W03G1.5 and AC3.3

enhanced the partial dauer arrest phenotype of *daf-8* (*e1393*) animals, RNAi of C37C3.6a and F59A2.3 enhanced the partial dauer arrest phenotype of *daf-14*(*m77*) animals, and RNAi of R05F9.10 enhanced dauer formation in both *daf-8* and *daf-14* genetic backgrounds (Figures 3A and 3B). These findings are consistent with a role of each of these five interactome components in repressing dauer formation during normal development.

Altogether, the thirteen genetic interactions identified connect five of the known *daf-7*/TGF- β pathway genes (*daf-1*/TGF- β -RI, *daf-7*/TGF- β , *daf-8*/R-SMAD, *daf-14*/SMAD2, and *daf-12*/NHR) to nine genes encoding components of the protein interaction map.

Limitations of the Genetic Perturbation Analysis

Although the genetic perturbation analysis was successful in identifying genes modulating dauer formation and their genetic interactions with known *daf-7*/TGF- β pathway genes, it is likely that there are a significant number of additional genes and interactions within the interactome network that were not identified in our experiments. Our analysis is limited by the particular alleles of known *daf-7*/TGF- β pathway mutants used as well as by the shortcomings of RNAi as a mode of gene inactivation. The penetrance of RNAi effects can be quite variable and is frequently significantly weaker than that of a corresponding genetic mutant (Fraser et al., 2000). In addition, *C. elegans* RNAi is notoriously ineffective in neurons (Tavernarakis et al., 2000). Given that neuronal signaling regulates dauer formation in *C. elegans* (Bargmann and Horvitz, 1991; Birnby et al., 2000; Li et al., 2003; Ren et al., 1996; Schackwitz et al., 1996; Wolkow et al., 2000), it is possible that many components of the interactome map might not score positively in our RNAi-based analysis.

In a series of control experiments, we used RNAi to inactivate 12 genes known to have an enhanced dauer arrest loss-of-function phenotype based on published phenotypes of genetic mutants. RNAi reproduced the expected phenotype in only three cases, and in each case the phenotype observed was weaker than that reported for the corresponding genetic mutant (data not shown). Therefore, we believe that the 9 genes and 13 genetic interactions identified in our experiments (Figure 3) represent a conservative estimate of the number of Y2H interactors that have *daf-7*/TGF- β pathway regulatory functions. Given that a genome-scale gene knockout project is underway in *C. elegans*, the availability of genetic mutants corresponding to all of the interactome components may allow a deeper functional analysis of *daf-7*/TGF- β signaling in the future.

An Integrated Protein and Genetic Interaction Map of the DAF-7/TGF- β Signaling Network

We combined the results of interactome mapping and systematic genetic perturbation analysis to construct an integrated map of the DAF-7/TGF- β signaling network (Figure 4). This map captures potential physical links based on Y2H interactions (Figure 4; gray links) or based on both Y2H and co-AP data (Figure 4; thicker black links), as well as functional relationships (Figure 4; links in red) derived from the results of genetic double pertur-

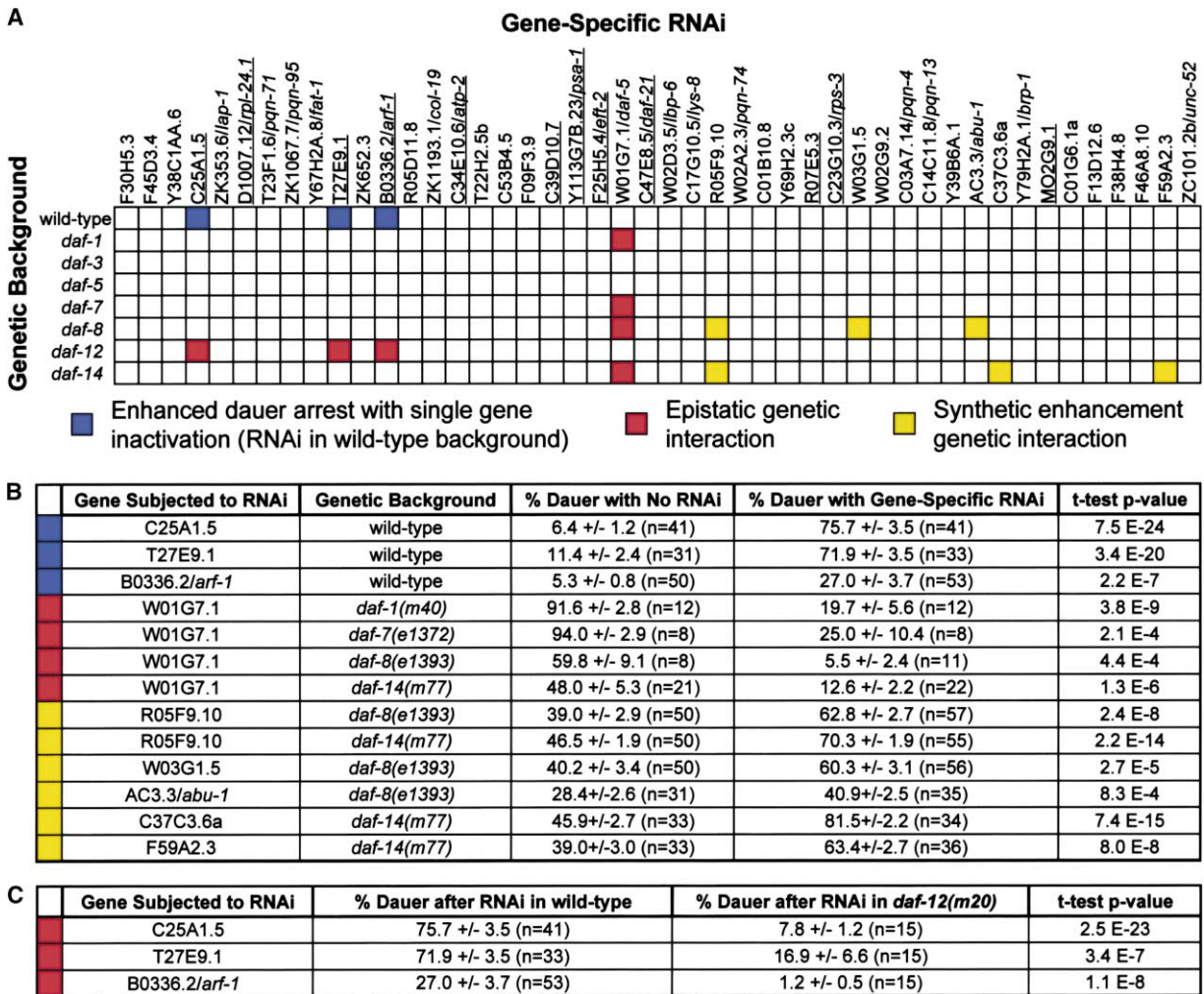


Figure 3. Single and Double Genetic Perturbation Experiments

(A) RNAi matrix. Loss-of-function genetic backgrounds are shown in rows, and genes subjected to RNAi are represented in columns. Unshaded boxes represent combinations that did not yield a statistically significant (i.e., $p < 0.001$ using Student's t test) effect on the frequency of dauer arrest when compared to "no RNAi" control experiments done in parallel. Shaded boxes denote statistically significant effects on dauer arrest frequency, with each color representing a phenotype or genetic interaction as indicated. Genes for which additional phenotypes (e.g., embryonic lethality, sterility, or nondauer larval arrest) were observed at varying degrees of penetrance are underlined. In each of these cases, our observations were consistent with similar developmental phenotypes previously reported in large-scale RNAi screens (Fraser et al., 2000; Gonczy et al., 2000; Kamath et al., 2003; Maeda et al., 2001; Piano et al., 2000).

(B and C) Numerical data from genetic perturbation experiments yielding statistically significant results (shaded boxes in [A]). Every experiment was carried out with multiple trials on multiple days. "No RNAi" indicates that animals were fed with bacteria containing the RNAi feeding vector pL4440 without an insert. In each trial, dauers and nondauers were counted. The average % dauer arrest \pm standard error of the mean (SEM) is listed, along with the total number of wells assayed (n) for each RNAi clone (see Experimental Procedures for details). In (B), the p value reflects the statistical significance of the difference in % dauer arrest in the no RNAi group compared to the gene-specific RNAi group. For the three experiments in (C), the p value reflects the statistical significance of the difference in dauer formation observed with gene-specific RNAi in the wild-type background compared to that observed with gene-specific RNAi in the *daf-12* loss-of-function background. Control and gene-specific RNAi phenotypes were calculated from animals assayed on the same 24 well plates to minimize artifacts of interplate variability (see Experimental Procedures for details).

bation experiments. Functional roles of components are indicated by pink or green colors (i.e., inhibition or activation, respectively, of dauer formation in the wild-type state) as inferred from genetic perturbation data (Figure 3). Seven of the nine modulators appear to be conserved in humans (Table 1); some of these may represent TGF- β signaling modulators in mammals. We cannot rule out the possibility that AC3.3/ABU-1 and W03G1.5 may have homologs that modulate TGF- β signaling in humans but are not identifiable by BLASTP-based homology searches.

Such integration of physical and genetic interactions for DAF-7/TGF- β signaling points to a higher level of complexity than is encompassed by current models. First, most physical interactions are part of a single connected network that includes both the DAF-1 and DAF-4 TGF- β receptors and the DAF-3/SMAD4 transcriptional regulator. Second, despite extensive forward genetic screens for additional members of DAF-7/TGF- β signaling (Inoue and Thomas, 2000; Malone and Thomas, 1994; Riddle et al., 1981; Thomas et al., 1993), the analy-

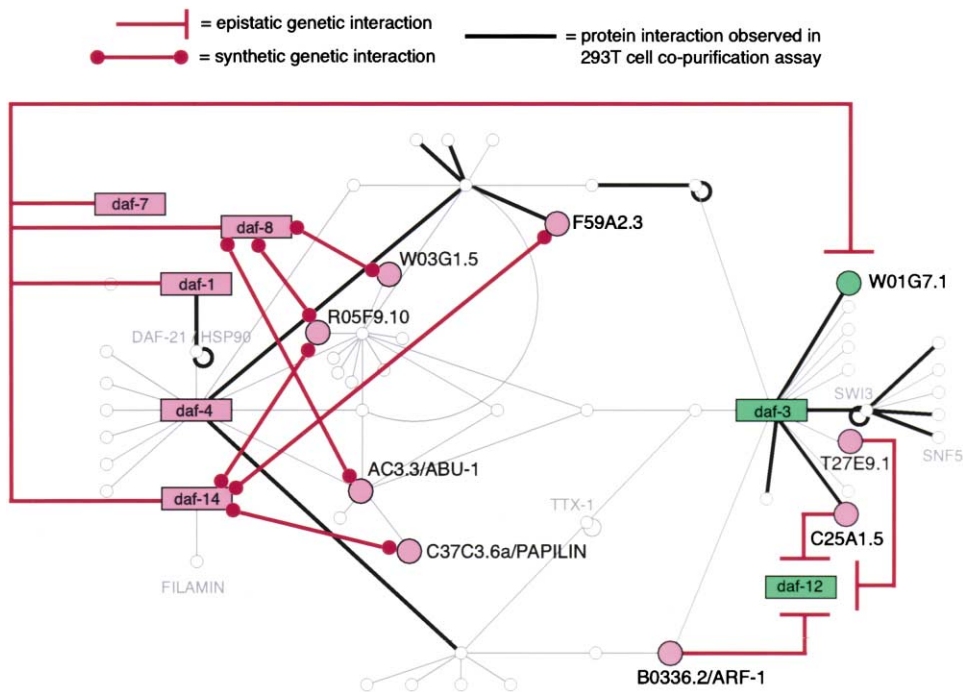


Figure 4. Integrated Map of a DAF-7/TGF- β Network

Y2H interactions and interactions observed in 293T cell copurification assays are shown together with genetic interactions detected from the double perturbation matrix. Known *daf-7*/TGF- β pathway genes and their products are in rectangular boxes and are labeled using an unitalicized lower case version of the standard *C. elegans* three-letter system to reflect the fact that the diagram combines both physical interactions between proteins and genetic interactions between genes. Physical interactions defined by Y2H data are represented as links in light gray. Those that have been tested and confirmed by co-AP assays are shown as thicker black lines. Genes and proteins that exhibited both Y2H and genetic interactions are indicated as large colored circles. Genes inferred to function to repress dauer formation in the wild-type state are indicated in pink, whereas those that act to induce dauer arrest in the wild-type state are indicated in green. Putative inhibitory relationships as inferred from epistasis analysis are indicated by red stopped arrows. The red dot-flanked lines correspond to the synthetic enhancement class of genetic interactions mapped in this study.

sis presented here identified numerous additional modifiers. Considering the false negative rates of both HT-Y2H and RNAi studies, it is possible that DAF-7/TGF- β signaling is mediated by an even greater number of components. Finally, we have started a thorough analysis of individual components identified here according to a prioritization scheme that gives the highest priority to components with both Y2H and co-AP evidence for physical interaction and data on genetic interaction with known DAF-7/TGF- β signaling factors. For example, W01G7.1 and C25A1.5 are of high priority given that they both interact with a known component of the pathway

(DAF-3/SMAD4) in Y2H and co-AP assays and also have genetic interactions with other known DAF-7/TGF- β pathway component(s). Below we provide in-depth evidence that one of them, W01G7.1, encodes a DAF-7/TGF- β signaling gene product.

Characterization of W01G7.1 and Identification of the Genetic Defect in *daf-5* Mutant Animals

Given that there are several uncloned but genetically mapped and characterized loci that modulate *daf-7*/TGF- β signaling, we asked whether proteins from our interactome network might be encoded by any of these

Table 1. Candidate Human Homologs of Modulators of *daf-7*/TGF- β Pathway Signaling

<i>C. elegans</i> ORF Name	Candidate Human Homolog	BLASTP e Value
T27E9.1	mitochondrial solute carrier family 25	1.00E-103
B0336.2/ <i>arf-1</i>	ADP-ribosylation factor 1	2.00E-96
C37C3.6	papilin	1.00E-76
C25A1.5	fatty acid hydroxylase domain containing 1	7.00E-63
R05F9.10	hypothetical protein DKFZp586N1020.1	2.00E-40
F59A2.3	tat-associated protein	2.00E-07
W01G7.1	SNO	2.80E-01
AC3.3/ <i>abu-1</i>	-	N/A
W03G1.5	-	N/A

C. elegans ORF names (along with gene names if available) are indicated along with candidate human homologs of the predicted *C. elegans* proteins as identified by BLASTP analysis.

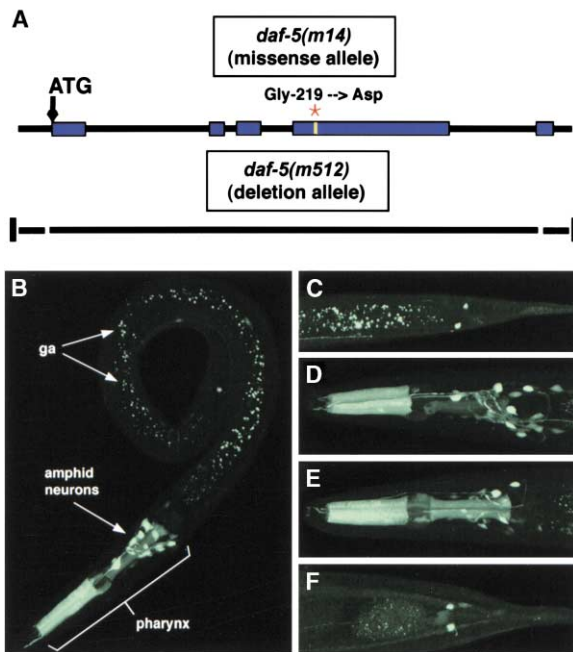


Figure 5. Characterization of W01G7.1/*daf-5*
 (A) Molecular identification of *daf-5* as W01G7.1. The *daf-5(m14)* allele carries a GGC to GAC change resulting in a Gly to Asp substitution at amino acid 219 in exon 4 of W01G7.1. The *m512* allele corresponds to a deletion of W01G7.1.
 (B–F) Expression pattern of W01G7.1/*daf-5* in *mEx127*.
 (B) L2 larva showing expression in anterior pharynx and head neurons. ga, gut autofluorescence.
 (C) L2 larva showing gut autofluorescence and GFP expression in tail neurons.
 (D and E) Adult expression patterns showing variability in posterior pharyngeal expression.
 (F) Expression in the adult tail.

loci. We noted that W01G7.1, a protein found to interact with DAF-3/SMAD4 (Figures 1B and 2), is encoded by a gene on the right arm of chromosome II in the vicinity of *daf-5*, a gene characterized by a forward genetic screen (Riddle et al., 1981). In addition, the genetic interaction pattern of W01G7.1 observed in the double genetic perturbation experiments (i.e., suppression of dauer arrest in *daf-1/TGF- β -RI*, *daf-7/TGF- β* , *daf-8/R-SMAD*, and *daf-14/SMAD2* backgrounds; Figures 3A and 3B) is identical to that reported for *daf-5* mutants (Thomas et al., 1993).

We performed independent mapping and molecular characterization of the genetic defect in *daf-5* mutant animals and found distinct mutations in W01G7.1 in two independent alleles of *daf-5*, *m14* and *m512* (Figure 5A). The ethyl methane sulfonate-induced *m14* allele carries a GGC to GAC change resulting in a Gly to Asp substitution at amino acid 219. The *m512* allele was isolated as a spontaneous suppressor of *daf-1(m412)* in a Tc1 mutator background (Yeh, 1991) and was presumed to be the result of a Tc1 insertion into *daf-5*. However, Southern hybridizations and PCR amplification of flanking genomic DNA showed that W01G7.1 but neither flanking gene is deleted in this *daf-5* mutant strain (data not shown; Experimental Procedures). Cosmid transfor-

mation rescue experiments further supported the conclusion that W01G7.1 corresponds to the *daf-5* gene (data not shown; Experimental Procedures).

The Tissue Expression Pattern of W01G7.1 is Consistent with a Role in the DAF-7/TGF- β Pathway

To investigate further the potential sites of action of W01G7.1/*daf-5* in the whole animal, we determined the tissue expression pattern of this gene by generating *C. elegans* strains carrying a GFP reporter driven by the W01G7.1/*daf-5* promoter. GFP expression was observed consistently in neurons in the head (including many amphid neurons and several unidentified cells located more anteriorly) and in neurons in the tail (Figures 5B–5F). W01G7.1/*daf-5* is not expressed in ASI, the amphid neuron pair in which *daf-7/TGF- β* is expressed (Ren et al., 1996; Schackwitz et al., 1996), consistent with its downstream role in the TGF- β signaling pathway. The most frequently observed neuron pair in the tail has been tentatively identified as the left and right LUA interneurons based on the extent and direction of infrequently observed cell processes. Faint expression was occasionally observed in two other neurons in the tail. W01G7.1/*daf-5* expression was also observed in the pharynx, most frequently in muscles in the anterior region (procorpus), but occasionally also in the isthmus and terminal bulb. Less frequently, expression in one or two cells located in the midbody was observed. By position, these could be ALML/R (touch-sensitive neurons), but no processes were observed.

Expression of the W01G7.1/*daf-5::GFP* transgene overlaps partially with that of the gene encoding its two-hybrid binding partner, DAF-3/SMAD4 (Patterson et al., 1997), and with that of *daf-1/TGF- β -RI* (Gunther et al., 2000) and *daf-4/TGF- β -RII* (Patterson et al., 1997). The overlap of W01G7.1/*daf-5* and *daf-3/SMAD4* expression occurs primarily in neurons in the head and in the pharynx (where W01G7.1/*daf-5* expression is stronger). Unlike *daf-3/SMAD4*, W01G7.1/*daf-5* is not expressed in the ventral cord, intestine, hypodermal cells, or gonadal distal tip cells. Cells in which W01G7.1/*daf-5* and *daf-1/TGF- β -RI* or W01G7.1/*daf-5* and *daf-4/TGF- β -RII* are expressed are confined to neurons in the head. W01G7.1/*daf-5*, *daf-3/SMAD4*, and *daf-4/TGF- β -RII* are expressed in the pharynx whereas *daf-1/TGF- β -RI* is not. *daf-3/SMAD4* and *daf-4/TGF- β -RII* are expressed in hypodermal cells; W01G7.1/*daf-5* and *daf-1/TGF- β -RI* are not. W01G7.1/*daf-5* and *daf-3/SMAD4* (Patterson et al., 1997), as well as *daf-1/TGF- β -RI* (Gunther et al., 2000), are expressed in midstage embryos, all larval stages, and the adult. Taken together, the data suggest that W01G7.1/DAF-5 functions in a complex with DAF-3 in neuronal and pharyngeal tissues to transduce the TGF- β signal regulating dauer formation.

W01G7.1/DAF-5 Has Structural and Functional Similarity to Human Sno/Ski Proteins

A sequence similarity search of putative and known protein sequences in the NCBI databases showed that W01G7.1/DAF-5 has similarity to the human SNO and SKI proteins (Figure 6A). SKI is a protooncogene encoded by the cellular counterpart of the avian tumor virus oncogene *v-ski* (Li et al., 1986; Nomura et al., 1989;

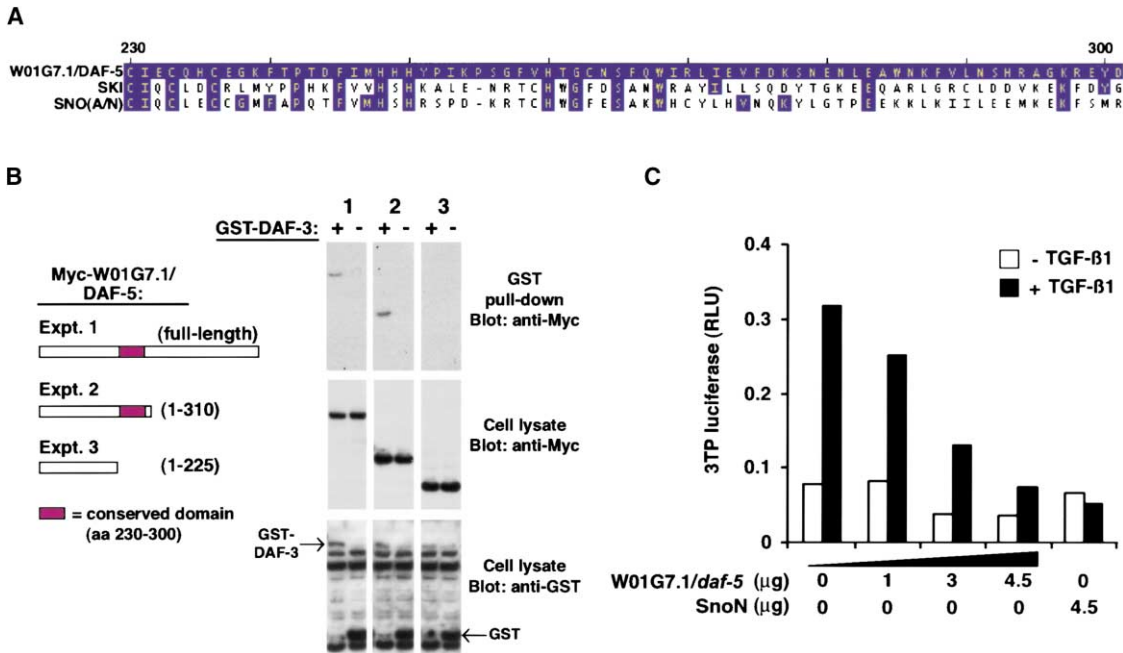


Figure 6. W01G7.1/DAF-5 Is Functionally Homologous to Human SNO/SKI Oncoproteins

(A) Region of amino acid sequence similarity of *C. elegans* W01G7.1/DAF-5 to human SNO and SKI proteins. SNOA and SNON are two isoforms of SNO that arise from alternative splicing of the Sno transcript. Their amino acids are identical within this region. Amino acids in SNO or SKI proteins identical to aligned amino acids in W01G7.1/DAF-5 are shaded in blue.

(B) The domain of W01G7.1/DAF-5 that interacts with DAF-3 maps to the region of amino acid sequence conservation with SNO/SKI. 293T cells were transfected with a GST-DAF-3 (+) or GST alone (-) expression plasmid along with various Myc-tagged W01G7.1/DAF-5 constructs as indicated. Cell lysates were subjected to affinity-purification using glutathione-Sepharose followed by immunoblotting with anti-Myc antibody (top panels). Aliquots of cell lysates were also subjected to immunoblotting to detect expression of Myc- and GST-tagged proteins (middle and lower panels, respectively).

(C) W01G7.1/DAF-5 represses TGF- β -induced transcription of the 3TP-luciferase reporter construct. HepG2 cells were cotransfected with 3TP-lux reporter plasmid together with empty pCMV-Myc-Dest expression vector, increasing amounts of a Myc-W01G7.1/DAF-5 construct, or a Myc-SNON construct as indicated. Cells were stimulated with TGF- β 1 (black bars) or left untreated (white bars). Luciferase activity is displayed in relative luciferase units (RLU; see Experimental Procedures).

Stavnezer et al., 1981, 1986). The SNO gene was originally isolated by screening human cDNA libraries with a *v-ski* cDNA probe and encodes a protein that is highly similar to SKI in amino acid sequence (Nomura et al., 1989). Multiple isoforms (i.e., SNON, SNOA, SNOI) arising from alternative splicing have been described (Nomura et al., 1989; Pearson-White, 1993).

SNO and SKI proteins physically associate with SMAD4 in a protein complex that functions in TGF- β signaling in mammalian cells (Macias-Silva et al., 2002; Stroschein et al., 1999). The sequence similarity of W01G7.1/DAF-5 to SNO/SKI and its physical interaction with DAF-3/SMAD4 supports the hypothesis that the SNO/SKI components of mammalian TGF- β signaling (Luo et al., 1999; Shinagawa et al., 2000; Stroschein et al., 1999) are conserved functionally throughout metazoa.

Strikingly, the region of sequence conservation between W01G7.1/DAF-5 and SKI corresponds to the region of SKI (and SNO) that physically interacts with the SMAD4 protein as demonstrated in a SKI/SMAD4 crystal structure (Wu et al., 2002). This indicates that a key structural domain is conserved between W01G7.1/DAF-5 and SNO/SKI (Figure 6A). To test this hypothesis experimentally, we generated expression plasmids encoding two C-terminal truncations of W01G7.1/DAF-5. One of the constructs encodes amino acids 1–310 of

W01G7.1/DAF-5, which retains the conserved region, whereas the other encodes amino acids 1–225, in which the conserved domain is absent (Figure 6B). When coexpressed with GST-DAF-3 in 293T cells, both full-length W01G7.1/DAF-5 and W01G7.1/DAF-5(1–310) associated specifically with GST-DAF-3, whereas the W01G7.1/DAF-5(1–225) protein fragment failed to bind. This suggests that the limited region of amino acid similarity between W01G7.1/DAF-5 and SNO/SKI contains a functionally important domain required for physical interaction with the DAF-3/SMAD4 protein.

To further explore functional similarity between W01G7.1/DAF-5 and SNO/SKI, we examined the ability of W01G7.1/DAF-5 to repress TGF- β -mediated transcriptional activation in HepG2 cells. Overexpression of SNON is known to repress TGF- β -mediated transcriptional activation of the p3TP-lux reporter construct (Stroschein et al., 1999; Wrana et al., 1992). We found that expression of increasing amounts of W01G7.1/DAF-5 in HepG2 cells decreased luciferase activity driven by the 3TP promoter upon TGF- β stimulation compared to cells transfected with vector alone (Figure 6C). The magnitude of the repression seen when 4.5 μ g of W01G7.1/DAF-5 expression plasmid was transfected was comparable to the degree of repression observed when the same amount of SNON expression plasmid

was transfected (Figure 6C). These results demonstrate that, like SNON, W01G7.1/DAF-5 can function as a transcriptional repressor of a TGF- β -responsive promoter.

Sno and *Smad4* knockout mice share the same phenotype, in that both exhibit enhanced tumor formation (Shinagawa et al., 2000; Takaku et al., 1999). Similarly, in our genetic experiments, W01G7.1/*daf-5* and *daf-3/SMAD4* loss-of-function mutants had the same phenotype, in that both were defective in dauer formation (Thomas et al., 1993). This highlights yet another functional similarity between W01G7.1/DAF-5 and SNO. Taken together, our findings support the assertion that W01G7.1/DAF-5 represents a *C. elegans* functional homolog of human SNO/SKI.

Other Modifiers of DAF-7/TGF- β Signaling Identified Here

Aside from W01G7.1/DAF-5, none of the other eight identified proteins (Table 1) have known roles in TGF- β signaling in *C. elegans* or in other species. One of these proteins, encoded by B0336.2, is a *C. elegans* homolog of human ADP-ribosylation factor 1 (ARF1) and interacts with DAF-3/SMAD4 in our two-hybrid assays (Figure 1B). Notably, in mammalian cells it has been observed that chemical inhibition of ADP-ribosyltransferases blocks TGF- β -induced gene expression (Beckmann et al., 1992). Our findings suggest that a physical association between ARF-1 and SMAD4 may underlie this observation.

Another DAF-3/SMAD4 interactor, T27E9.1, encodes a protein with strong amino acid sequence similarity to mammalian proteins of the mitochondrial solute carrier family 25 (Figure 1B; Table 1). A member of this family, *Slc25a4*, is an adenine nucleotide transporter that can induce apoptosis (Bauer et al., 1999). Given the known ability of TGF- β to modulate apoptosis, direct association of SMAD4 with mitochondrial adenine nucleotide transporters could be part of the mechanism by which TGF- β regulates cell death.

R05F9.10 encodes a protein that contains three TPR repeats and is linked to DAF-4/TGF- β -RII through an intermediate interactor (Figure 1B; Table 1). TPR domains mediate interactions with the carboxy termini of many proteins, including the chaperone Hsp90 (Blatch and Lassle, 1999; Young et al., 1998). Our finding that the *C. elegans* Hsp90 homolog DAF-21 also physically interacts with DAF-4/TGF- β -RII (Figure 1B) suggests that a receptor-associated protein complex containing DAF-21/Hsp90 and the R05F9.10 protein might regulate DAF-7/TGF- β -like signal transduction.

The DAF-4/TGF- β -RII binding protein AC3.3/ABU-1 is a transmembrane protein whose synthesis is induced in mutant animals that are defective in the unfolded protein response (Urano et al., 2002). ABU-1 localizes to the endoplasmic reticulum (ER) when expressed in mammalian cells (Urano et al., 2002). Taken together with the enhancement of *daf-8(e1393)* dauer phenotypes by RNAi of AC3.3/*abu-1* (Figures 3A and 3B), this observation suggests a model whereby AC3.3/ABU-1 could potentiate DAF-7/TGF- β signaling by facilitating trafficking of DAF-4/TGF- β -RII from the ER to the plasma membrane.

C37C3.6a, which has a synthetic enhancement inter-

action with *daf-14(m77)* in double perturbation experiments (Figures 3A and 3B), is predicted to encode a protein with thrombospondin and trypsin inhibitor domains. The association of C37C3.6a with the ER resident protein AC3.3/ABU-1 (Figure 1B) suggests that it may also play a role in DAF-4/TGF- β -RII trafficking. Interestingly, human ADAMTS-2, a close mammalian homolog of C37C3.6a, is transcriptionally induced 8-fold by TGF- β (Wang et al., 2003), suggesting the existence of a feed-forward mechanism involving C37C3.6a that could facilitate proper trafficking of DAF-4/TGF- β -RII.

Conclusions

To our knowledge, this is the first report of integrating large-scale protein interaction mapping with systematic multiple genetic perturbations to study a metazoan signaling pathway. This strategy not only identified a component of *daf-7/TGF- β* signaling that was independently confirmed by traditional forward genetic analysis (i.e., W01G7.1/*daf-5*) but also identified eight other *daf-7/TGF- β* pathway modulators that have eluded identification by more conventional approaches. Given the relative insensitivity of RNAi in reproducing phenotypes of known dauer mutants (as discussed previously; data not shown), this represents a conservative estimate of the number of modulators of DAF-7/TGF- β signaling identified in this study. As most of these modulators appear to be conserved in the human genome, they may open new avenues of investigation for understanding human TGF- β signaling and its dysregulation in disease. Our results indicate that combining interactome maps with systematic multiple perturbation methods can identify biologically relevant components and contribute to a better understanding of the logic of molecular networks. Such an approach may be useful for studying biological processes at the systems scale.

Experimental Procedures

ORF Cloning and Yeast Two-Hybrid Screening

ORFs were gateway cloned as described (Reboul et al., 2001). Proteome-wide Y2H screens were performed as described (Walhout and Vidal, 2001a) using the AD-wrmcDNA library (Walhout et al., 2000b). Typically, 1–3 million transformants were screened for each bait. In the first-generation screens, DAF-8/R-SMAD could not be used, because a DB-DAF-8 fusion behaved as an autoactivator in the system. To minimize experimental false positive interactions, we utilized a version of the two-hybrid system that expresses baits and preys from low copy number plasmids. We also systematically discarded a few AD-cDNA fusions detected with many other baits in other Y2H screens unrelated to the DAF-7/TGF- β pathway and thus considered as spurious interactors. Finally, we rigorously retested all interactions in fresh yeast cells to eliminate false positive interactions arising from spurious autoactivators or any other mutational events.

For use in second-generation screens, full-length predicted open reading frames (ORFs) corresponding to Y2H interactors obtained from the initial screens were amplified from a mixed-stage *C. elegans* cDNA library and cloned as previously described (Reboul et al., 2001). This procedure successfully cloned ORFs corresponding to 21 of the 28 “first-generation” interactors (Supplemental Table S1, available on *Molecular Cell's* website). These were then subcloned as DB-X fusions using the Gateway system. Two of the DB-ORF fusions (DB-R05D11.8 and DB-ZK1193.1) behaved as autoactivators and could not be used in screens. The remaining 19 baits were screened against the AD-wrmcDNA library to identify second-

generation interactors. These interactions were also retested in the same manner as described above for first-generation interactions.

RNAi and Assays for Dauer Arrest

Feeding RNAi constructs were constructed as previously described (Boulton et al., 2002) or obtained from the Ahringer genomic RNAi library (Kamath et al., 2003). Sequence-verified feeding RNAi clones were successfully obtained for 46 out of 55 (84%) of the interactors (Supplemental Table S3, available on *Molecular Cell's* website). Feeding RNAi was performed as previously described (Boulton et al., 2002) with the following modifications. Single L4 animals were picked to wells in 24 well plates containing NGM agar + 5 mM IPTG and HT115(DE3) bacteria carrying double-stranded RNA expression constructs and allowed to develop for ~24 hours at 15°C. Animals were shifted to the assay temperature (25°C or 27°C) when gravid, and the P₀ animals were removed 14–18 hr later. Progeny (typically 20–100 animals per well) were assayed for the dauer phenotype approximately 48 hr thereafter. Wells in which fewer than ten progeny were available for assay were not included in the analysis. Dauer assays in wild-type animals were done at 27°C, and those in mutant backgrounds were generally conducted at 25°C. The exception is that genes that produced enhanced dauer arrest phenotypes at 27°C in wild-type animals were tested for genetic interaction with *daf-12(m20)* at 27°C. Dauers and reproductively growing animals were counted under dissecting microscopes. Dauer arrest RNAi phenotypes at 27°C were confirmed by visualization of dauer alae using differential interference contrast microscopy. *p* values were calculated using Student's *t* test (two tailed, two sample, unequal variance). Wild-type animals used were the Bristol N2 strain. Loss-of-function mutants corresponded to the following alleles: *daf-1(m40)*, *daf-3(e1376)*, *daf-5(e1386)*, *daf-7(e1372)*, *daf-8(e1393)*, *daf-14(m77)*, and *daf-12(m20)*.

In all experiments, every RNAi clone was assayed in at least quadruplicate (four wells per RNAi clone), and each 24 well plate contained both positive and negative RNAi controls in quadruplicate. This was done to minimize the substantial variability in population dauer phenotypes among animals with intermediate dauer phenotypes (Ailion and Thomas, 2000). We frequently observed such variability among animals of the same genetic background that were assayed on separate 24 well plates in the same incubator on the same day. By including positive and negative controls on each 24 well plate, we were able to control for interplate phenotypic variability and limit phenotypic comparisons to those animals that were assayed on the same plate. For assays performed at 27°C and in the *daf-8(e1393)* and *daf-14(m77)* genetic backgrounds, all RNAi clones yielding statistically significant effects were retested with negative control RNAi and test RNAi in multiple wells (10 to 11 wells per RNAi clone) per 24 well plate.

Genetic Mapping of *daf-5*

daf-5 was mapped by recombination to a position between *rol-1* and *unc-52*, using suppression of the temperature-sensitive Daf-c (dauer constitutive) phenotype of *daf-7(e1372)* as an assay for the presence of *daf-5*.

Finer resolution mapping was carried out using DNA dimorphisms in this region (A.M. Schaefer, J. Jakubowski, K. Kornfeld, and M.L. Nonet, personal communication) between the wild-type strains N2 and RC301 (Hodgkin and Doniach, 1997) as scorable markers in two different ordering crosses. The dimorphisms were detected by PCR as products of different length from the two strains and can thus be scored either in homozygotes or heterozygotes. Suppression of *daf-7(e1372)* was again used as an assay for the presence of *daf-5*.

Primer sequences for detection of DNA dimorphisms were as follows: *jsP304*, 5'-GTCCCCAAGCAATCTACAAATATG-3' and 5'-GACTTCTCGGTTATCACCCGCC-3'; *jsP305*, 5'-CTGCGAACACTCTCATAATCCGTCC-3' and 5'-CCGTTGTTTGACCTTACAAATTAAC-3'; *jsP307*, 5'-CAGCCAGCGTAGCTAGCAATCGGAG-3' and 5'-CGGAGCTCTT CGAGGAGCACAACG-3'.

Germline Transformation and Cosmid Rescue Experiments

Transgenic lines were generated as described (Mello et al., 1991). Young adult *daf-5(e1386)*; *daf-7(e1372)* hermaphrodites were immobilized on dried agarose pads under halocarbon oil and injected

with a 1:1 mixture of selectable marker and test DNA in 1× injection buffer (total DNA concentration, 200 ng/ μ l). Cosmid W01G7 was used for transformation rescue experiments using cloned *rol-6(su1006)* DNA as a coinjection marker. DNA for W01G7 and another cosmid in this region, W02B8, was prepared from cosmid clones (gift of Alan Coulson) using a Qiagen midi-prep kit. Four stably transmitting lines were established for W01G7, and these were scored for rescue of *daf-5* using abolishment of *daf-5* suppression of the *daf-7 Daf-c* (dauer constitutive) phenotype at 25°C as an assay. As a control, one line was obtained for another cosmid in this region, W02B8. *daf-5* was not rescued in the W02B8 line, whereas four W01G7 lines exhibited complete rescue, indicating that W01G7 carries the wild-type *daf-5* gene.

Sequencing of *daf-5* Mutant Alleles

DNA sequence for *daf-5* mutations was derived either from multiple cloned fragments (generated by PCR and cloned into pGEM-T vectors) or directly from PCR products. PCR amplifications were performed using high-fidelity DNA polymerase (BRL Platinum Taq HF) under conditions specified by the manufacturer.

Southern Analysis of Genomic DNA from *daf-5* Mutant Animals

A nearly full-length cDNA (yk130g8, approximately 2.7 kb) corresponding to W01G7.1 was obtained from a lambda-ZAP clone provided by Yuji Kohara. The derived pBluescript plasmid insert was partially sequenced from both ends using M13 oligonucleotide primers. Approximately 10 μ g of purified DNA from the yk130g8 pBluescript clone was digested overnight with PstI, generating two fragments containing insert DNA (1133 bp and 600 bp). These fragments were gel purified, pooled, extracted, and radiolabeled with ³²P dCTP using the random hexamer method. Approximately 10 μ g each of purified genomic DNAs from N2, *daf-5(m512)*, and *daf-1(m412::Tc1)* (the mutator parent of *m512*) were digested overnight with XbaI and resulting fragments were resolved by agarose gel electrophoresis along with BstEII-digested lambda marker DNA and transferred to a nitrocellulose membrane. The membrane was incubated with radiolabeled yk130g8 fragments and exposed to X-ray film.

Localization of W01G7.1/*daf-5* Expression Using a GFP Fusion Transgene

A 3855 bp fragment of W01G7.1 genomic DNA containing 2563 bp of 5' sequence, exon 1, and part of exon 2 was cloned into the GFP expression vector pPD95.75 (without a nuclear localization signal) and coinjected into the germline of N2 with the dominant *rol-6* transformation marker to produce a line of genotype *mEx127[daf-5::gfp rol-6(su1006)]*. This extrachromosomal transgene was integrated into chromosomal DNA by exposure to gamma radiation. Two independent lines (*mIs19* and *mIs20*) were established after resegregation from wild-type. GFP expression patterns in all three strains were very similar.

HepG2 Cell Transfections and 3TP-Lux Reporter Assays

HepG2 cells were transfected with 0.25 μ g of the 3TP-lux luciferase reporter plasmid (Wrana et al., 1992), 50 ng of the β -galactosidase reporter plasmid pCH110 (obtained from Pharmacia-LKB; containing a *lacZ* gene under the control of the SV40 early region promoter), and varying amounts of the gene expression construct under study. Gene expression vector plasmid without a gene insert was included in the transfection to make the total gene expression construct DNA equal to 4.5 μ g. Cells were cultured and transfected in 6 well tissue culture plates in 2 mL Opti-MEM using Lipofectamine Plus (Invitrogen) according to the manufacturer's instructions. The cells were washed with serum-free medium and incubated with 2.5 ng/ml of purified recombinant human TGF- β 1 (R&D Systems Inc., Minneapolis, MN) in serum-free medium 24 hr following the transfections. Luciferase and β -galactosidase activities were measured according to manufacturer's instructions (Tropix, Bedford, MA) after 16–20 hr of TGF- β stimulation. The activity of β -galactosidase was used to correct variation in transfection efficiencies between wells by calculating a relative luciferase activity (luciferase value/ β -galactosidase value; expressed as relative luciferase units). The experiments were repeated at least three times with similar findings.

Co-AP Experiments in 293T Cells

We Gateway cloned full-length ORFs corresponding to proteins comprising 51 of the 71 predicted protein interactions in the interactome network (see ORF cloning section above). Entry clones of bait proteins were subcloned into pDEST-27 (Invitrogen), which contained the GST coding sequence upstream of a Gateway recombination site. Entry clones of prey proteins were subcloned into pCMV-Myc-DEST, which contains a Myc epitope tag upstream of the Gateway recombination site (Xu et al., 2003). Both vectors express their respective fusion polypeptides from a CMV promoter. Constructs encoding W01G7.1/DAF-5 truncations were generated by PCR, Gateway cloned, and sequence verified. For co-AP experiments, 1.5 μ g of each plasmid was transfected into 293T cells using Lipofectamine 2000 reagent according to the manufacturers instructions (Invitrogen). For GST control plasmids, 0.5 μ g was used per transfection because we found that higher amounts significantly reduced expression of the cotransfected Myc-tagged ORF. Cells were cultured for 2 days in DMEM medium with 10% fetal bovine serum (Invitrogen) and lysed in 0.5% NP-40 buffer (20 mM Tris-HCl [pH 8.0], 100 mM NaCl, 1 mM EDTA, and complete protease inhibitor cocktail [Amersham]). Lysates were cleared by centrifugation at $14,000 \times g$ before precipitation of protein complexes using glutathione-Sepharose beads. Beads were washed three times with lysis buffer, and purified complexes and control lysate samples were separated on NuPAGE acrylamide gels (Invitrogen). Myc- and GST-tagged proteins were detected using standard immunoblotting techniques. Antibodies used were mouse monoclonal anti-Myc (clone 9E10) and rabbit polyclonal anti-GST from Sigma.

Each of the 51 interactions was tested in the co-AP assay. In 32 cases the experiment results were not interpretable either because (a) expression of the Myc-tagged prey protein was undetectable in cell lysates following transfection, (b) the Myc-tagged prey protein was not expressed at comparable levels in the GST-bait transfection as compared to the GST control transfection, (c) expression of the GST-bait protein could not be detected, or (d) the Myc-prey protein bound nonspecifically to GST protein alone. Similar protein expression success rates have been observed by us and others in the context of high-throughput settings (Braun et al., 2002; Reboul et al., 2003). Nevertheless, the assay results were interpretable for 19 protein-protein interaction pairs, as comparable expression levels of Myc-tagged prey protein were obtained between GST-bait and GST transfections, and GST-bait protein expression was detectable.

Acknowledgments

We thank Cathy Gunther, Peifeng Ren, Sharon Cantor, David Hill, Denis Dupuy, Marian Walhout, Simon Boulton, Jérôme Reboul, and Shivapriya Ramaswamy for helpful discussions and advice; Roger Greenberg and David Hill for critical review of the manuscript; Suzanne Clark for technical assistance; Atisha Chatterjee for expert DNA sequencing; Alan Coulson for the gift of cosmid strains; Yuji Kohara and Garth Patterson for a W01G7.1/*daf-5* cDNA; Kunxin Luo and Yin Sun for SNON cDNA; William P. Shiemann for the p3TP-lux reporter plasmid; Julie Ahlinger for several RNAi feeding constructs; Andrew Fire for the GFP expression vector; and Anneliese Schaefer and Mike Nonet for primers used in the DNA dimorphism analysis. Some strains were provided by the *Caenorhabditis* Genetics Center (University of Minnesota, St. Paul). This work was funded by DHHS grant GM60151 (to D.L.R.), Physician Postdoctoral Fellowships from the Howard Hughes Medical Institute (to M.T. and P.J.H.), a Damon-Runyon Postdoctoral Fellowship (to M.T.), NIH awards K08-DK62884 (to P.J.H.) and K08-AG21613 (to M.T.), an EMBO Long-Term Fellowship (to P.-O.V.), and NIH grants 5R01HG01715-02 (NHGRI and NIGMS) and 7R33CA81658-02 (NCI) (to M.V.).

Received: September 8, 2003
Revised: December 16, 2003
Accepted: December 23, 2003
Published: February 26, 2004

References

Ailion, M., and Thomas, J.H. (2000). Dauer formation induced by high temperatures in *Caenorhabditis elegans*. *Genetics* 156, 1047–1067.

Antebi, A., Yeh, W.H., Tait, D., Hedgecock, E.M., and Riddle, D.L. (2000). *daf-12* encodes a nuclear receptor that regulates the dauer diapause and developmental age in *C. elegans*. *Genes Dev.* 14, 1512–1527.

Avery, L., and Wasserman, S. (1992). Ordering gene function: the interpretation of epistasis in regulatory hierarchies. *Trends Genet.* 8, 312–316.

Bargmann, C.I., and Horvitz, H.R. (1991). Control of larval development by chemosensory neurons in *Caenorhabditis elegans*. *Science* 251, 1243–1246.

Bauer, M.K., Schubert, A., Rocks, O., and Grimm, S. (1999). Adenine nucleotide translocase-1, a component of the permeability transition pore, can dominantly induce apoptosis. *J. Cell Biol.* 147, 1493–1502.

Beckmann, J.D., Illig, M., Romberger, D., and Rennard, S.I. (1992). Induction of fibronectin gene expression by transforming growth factor beta-1 is attenuated in bronchial epithelial cells by ADP-ribosyltransferase inhibitors. *J. Cell. Physiol.* 152, 274–280.

Birnbay, D.A., Link, E.M., Vowels, J.J., Tian, H., Colacurcio, P.L., and Thomas, J.H. (2000). A transmembrane guanylyl cyclase (DAF-11) and Hsp90 (DAF-21) regulate a common set of chemosensory behaviors in *caenorhabditis elegans*. *Genetics* 155, 85–104.

Blatch, G.L., and Lassle, M. (1999). The tetratricopeptide repeat: a structural motif mediating protein-protein interactions. *Bioessays* 21, 932–939.

Boulton, S.J., Gartner, A., Reboul, J., Vaglio, P., Dyson, N., Hill, D.E., and Vidal, M. (2002). Combined functional genomic maps of the *C. elegans* DNA damage response. *Science* 295, 127–131.

Braun, P., Hu, Y., Shen, B., Halleck, A., Koundinya, M., Harlow, E., and LaBaer, J. (2002). Proteome-scale purification of human proteins from bacteria. *Proc. Natl. Acad. Sci. USA* 99, 2654–2659.

Estevez, A.O. (1997). The role of the *daf-8* gene in *Caenorhabditis elegans* dauer larva development. PhD thesis, University of Missouri-Columbia, Columbia, Missouri.

Estevez, M., Attisano, L., Wrana, J.L., Albert, P.S., Massague, J., and Riddle, D.L. (1993). The *daf-4* gene encodes a bone morphogenetic protein receptor controlling *C. elegans* dauer larva development. *Nature* 365, 644–649.

Fraser, A.G., Kamath, R.S., Zipperlen, P., Martinez-Campos, M., Sohrmann, M., and Ahlinger, J. (2000). Functional genomic analysis of *C. elegans* chromosome I by systematic RNA interference. *Nature* 408, 325–330.

Ge, H., Walhout, A.J., and Vidal, M. (2003). Integrating “omic” information: a bridge between genomics and systems biology. *Trends Genet.* 19, 551–560.

Georgi, L.L., Albert, P.S., and Riddle, D.L. (1990). *daf-1*, a *C. elegans* gene controlling dauer larva development, encodes a novel receptor protein kinase. *Cell* 61, 635–645.

Gonczy, P., Echeverri, C., Oegema, K., Coulson, A., Jones, S.J., Copley, R.R., Duperon, J., Oegema, J., Brehm, M., Cassin, E., et al. (2000). Functional genomic analysis of cell division in *C. elegans* using RNAi of genes on chromosome III. *Nature* 408, 331–336.

Guarente, L. (1993). Synthetic enhancement in gene interaction: a genetic tool come of age. *Trends Genet.* 9, 362–366.

Gunther, C.V., Georgi, L.L., and Riddle, D.L. (2000). A *Caenorhabditis elegans* type I TGF beta receptor can function in the absence of type II kinase to promote larval development. *Development* 127, 3337–3347.

Hodgkin, J., and Doniach, T. (1997). Natural variation and copulatory plug formation in *Caenorhabditis elegans*. *Genetics* 146, 149–164.

Ideker, T., Galitski, T., and Hood, L. (2001). A new approach to decoding life: systems biology. *Annu. Rev. Genomics Hum. Genet.* 2, 343–372.

Inoue, T., and Thomas, J.H. (2000). Targets of TGF-beta signaling in *Caenorhabditis elegans* dauer formation. *Dev. Biol.* 217, 192–204.

Kamath, R.S., Fraser, A.G., Dong, Y., Poulin, G., Durbin, R., Gotta, M., Kanapin, A., Le Bot, N., Moreno, S., Sohrmann, M., et al. (2003). Systematic functional analysis of the *Caenorhabditis elegans* genome using RNAi. *Nature* 421, 231–237.

Kitano, H. (2002). Computational systems biology. *Nature* 420, 206–210.

- Klochendler-Yeivin, A., Muchardt, C., and Yaniv, M. (2002). SWI/SNF chromatin remodeling and cancer. *Curr. Opin. Genet. Dev.* 12, 73–79.
- Li, Y., Turck, C.M., Teumer, J.K., and Stavnezer, E. (1986). Unique sequence, ski, in Sloan-Kettering avian retroviruses with properties of a new cell-derived oncogene. *J. Virol.* 57, 1065–1072.
- Li, W., Kennedy, S.G., and Ruvkun, G. (2003). *daf-28* encodes a *C. elegans* insulin superfamily member that is regulated by environmental cues and acts in the DAF-2 signaling pathway. *Genes Dev.* 17, 844–858.
- Luo, K., Stroschein, S.L., Wang, W., Chen, D., Martens, E., Zhou, S., and Zhou, Q. (1999). The Ski oncoprotein interacts with the Smad proteins to repress TGF β signaling. *Genes Dev.* 13, 2196–2206.
- Macias-Silva, M., Li, W., Leu, J.J., Crissey, M.A., and Taub, R. (2002). Up-regulated transcriptional repressors SnoN and Ski bind Smad proteins to antagonize transforming growth factor- β signals during liver regeneration. *J. Biol. Chem.* 277, 28483–28490.
- Maeda, I., Kohara, Y., Yamamoto, M., and Sugimoto, A. (2001). Large-scale analysis of gene function in *Caenorhabditis elegans* by high-throughput RNAi. *Curr. Biol.* 11, 171–176.
- Malone, E.A., and Thomas, J.H. (1994). A screen for nonconditional dauer-constitutive mutations in *Caenorhabditis elegans*. *Genetics* 136, 879–886.
- Massague, J. (1998). TGF- β signal transduction. *Annu. Rev. Biochem.* 67, 753–791.
- Massague, J., Blain, S.W., and Lo, R.S. (2000). TGF β signaling in growth control, cancer, and heritable disorders. *Cell* 103, 295–309.
- Mello, C.C., Kramer, J.M., Stinchcomb, D., and Ambros, V. (1991). Efficient gene transfer in *C. elegans*: extrachromosomal maintenance and integration of transforming sequences. *EMBO J.* 10, 3959–3970.
- Nomura, N., Sasamoto, S., Ishii, S., Date, T., Matsui, M., and Ishizaki, R. (1989). Isolation of human cDNA clones of ski and the ski-related gene, sno. *Nucleic Acids Res.* 17, 5489–5500.
- Patterson, G.I., Kowek, A., Wong, A., Liu, Y., and Ruvkun, G. (1997). The DAF-3 Smad protein antagonizes TGF- β -related receptor signaling in the *Caenorhabditis elegans* dauer pathway. *Genes Dev.* 11, 2679–2690.
- Pearson-White, S. (1993). Sno1, a novel alternatively spliced isoform of the ski protooncogene homolog, sno. *Nucleic Acids Res.* 21, 4632–4638.
- Piano, F., Schetter, A.J., Mangone, M., Stein, L., and Kempthues, K.J. (2000). RNAi analysis of genes expressed in the ovary of *Caenorhabditis elegans*. *Curr. Biol.* 10, 1619–1622.
- Reboul, J., Vaglio, P., Tzellas, N., Thierry-Mieg, N., Moore, T., Jackson, C., Shin-i, T., Kohara, Y., Thierry-Mieg, D., Thierry-Mieg, J., et al. (2001). Open-reading-frame sequence tags (OSTs) support the existence of at least 17,300 genes in *C. elegans*. *Nat Genet* 27, 332–336.
- Reboul, J., Vaglio, P., Rual, J.F., Lamesch, P., Martinez, M., Armstrong, C.M., Li, S., Jacotot, L., Bertin, N., Janky, R., et al. (2003). *C. elegans* ORFeome version 1.1: experimental verification of the genome annotation and resource for proteome-scale protein expression. *Nat. Genet.* 34, 35–41.
- Ren, P., Lim, C.S., Johnsen, R., Albert, P.S., Pilgrim, D., and Riddle, D.L. (1996). Control of *C. elegans* larval development by neuronal expression of a TGF- β homolog. *Science* 274, 1389–1391.
- Riddle, D.L. (1988). The dauer larva. In *The Nematode Caenorhabditis elegans*, W.B. Wood, ed. (Plainview, NY: Cold Spring Harbor Laboratory Press), pp. 393–412.
- Riddle, D.L., Swanson, M.M., and Albert, P.S. (1981). Interacting genes in nematode dauer larva formation. *Nature* 290, 668–671.
- Sasaki, A., Masuda, Y., Ohta, Y., Ikeda, K., and Watanabe, K. (2001). Filamin associates with Smads and regulates transforming growth factor- β signaling. *J. Biol. Chem.* 276, 17871–17877.
- Satterlee, J.S., Sasakura, H., Kuhara, A., Berkeley, M., Mori, I., and Sengupta, P. (2001). Specification of thermosensory neuron fate in *C. elegans* requires *txx-1*, a homolog of *otd/Otx*. *Neuron* 31, 943–956.
- Schackwitz, W.S., Inoue, T., and Thomas, J.H. (1996). Chemosensory neurons function in parallel to mediate a pheromone response in *C. elegans*. *Neuron* 17, 719–728.
- Shinagawa, T., Dong, H.D., Xu, M., Maekawa, T., and Ishii, S. (2000). The sno gene, which encodes a component of the histone deacetylase complex, acts as a tumor suppressor in mice. *EMBO J.* 19, 2280–2291.
- Smith, D.B., and Johnson, K.S. (1988). Single-step purification of polypeptides expressed in *Escherichia coli* as fusions with glutathione S-transferase. *Gene* 67, 31–40.
- Stavnezer, E., Gerhard, D.S., Binari, R.C., and Balazs, I. (1981). Generation of transforming viruses in cultures of chicken fibroblasts infected with an avian leukosis virus. *J. Virol.* 39, 920–934.
- Stavnezer, E., Barkas, A.E., Brennan, L.A., Brodeur, D., and Li, Y. (1986). Transforming Sloan-Kettering viruses generated from the cloned *v-ski* oncogene by in vitro and in vivo recombinations. *J. Virol.* 57, 1073–1083.
- Stroschein, S.L., Wang, W., Zhou, S., Zhou, Q., and Luo, K. (1999). Negative feedback regulation of TGF- β signaling by the SnoN oncoprotein. *Science* 286, 771–774.
- Takaku, K., Miyoshi, H., Matsunaga, A., Oshima, M., Sasaki, N., and Taketo, M.M. (1999). Gastric and duodenal polyps in Smad4 (*Dpc4*) knockout mice. *Cancer Res.* 59, 6113–6117.
- Tavernarakis, N., Wang, S.L., Dorovkov, M., Ryazanov, A., and Driscoll, M. (2000). Heritable and inducible genetic interference by double-stranded RNA encoded by transgenes. *Nat. Genet.* 24, 180–183.
- Thatcher, J.D., Haun, C., and Okkema, P.G. (1999). The DAF-3 Smad binds DNA and represses gene expression in the *Caenorhabditis elegans* pharynx. *Development* 126, 97–107.
- Thomas, J.H., Birnby, D.A., and Vowels, J.J. (1993). Evidence for parallel processing of sensory information controlling dauer formation in *Caenorhabditis elegans*. *Genetics* 134, 1105–1117.
- Urano, F., Calfon, M., Yoneda, T., Yun, C., Kiraly, M., Clark, S.G., and Ron, D. (2002). A survival pathway for *Caenorhabditis elegans* with a blocked unfolded protein response. *J. Cell Biol.* 158, 639–646.
- Vidal, M. (1997). The reverse two-hybrid system. In *The Yeast Two-Hybrid System*, P.L. Bartel and S. Fields, eds. (New York: Oxford University Press), pp. 109–147.
- Vidal, M. (2001). A biological atlas of functional maps. *Cell* 104, 333–339.
- Walhout, A.J., and Vidal, M. (2001a). High-throughput yeast two-hybrid assays for large-scale protein interaction mapping. *Methods* 24, 297–306.
- Walhout, A.J., and Vidal, M. (2001b). Protein interaction maps for model organisms. *Nat. Rev. Mol. Cell Biol.* 2, 55–62.
- Walhout, A.J., Sordella, R., Lu, X., Hartley, J.L., Temple, G.F., Brasch, M.A., Thierry-Mieg, N., and Vidal, M. (2000a). Protein interaction mapping in *C. elegans* using proteins involved in vulval development. *Science* 287, 116–122.
- Walhout, A.J., Temple, G.F., Brasch, M.A., Hartley, J.L., Lorson, M.A., van den Heuvel, S., and Vidal, M. (2000b). GATEWAY recombinational cloning: application to the cloning of large numbers of open reading frames or ORFeomes. *Methods Enzymol.* 328, 575–592.
- Walhout, A.J., Reboul, J., Shtanko, O., Bertin, N., Vaglio, P., Ge, H., Lee, H., Doucette-Stamm, L., Gunsalus, K.C., Schetter, A.J., et al. (2002). Integrating interactome, phenome, and transcriptome mapping data for the *C. elegans* germline. *Curr. Biol.* 12, 1952–1958.
- Wang, W.M., Lee, S., Steigltz, B.M., Scott, I.C., Lebares, C.C., Allen, M.L., Brenner, M.C., Takahara, K., and Greenspan, D.S. (2003). Transforming growth factor- β induces secretion of activated ADAMTS-2. A procollagen III N-proteinase. *J. Biol. Chem.* 278, 19549–19557.
- Wolkow, C.A., Kimura, K.D., Lee, M.S., and Ruvkun, G. (2000). Regulation of *C. elegans* life-span by insulinlike signaling in the nervous system. *Science* 290, 147–150.
- Wrana, J.L., Attisano, L., Carcamo, J., Zentella, A., Doody, J., Laiho, M., Wang, X.F., and Massague, J. (1992). TGF β signals through a heteromeric protein kinase receptor complex. *Cell* 71, 1003–1014.
- Wu, J.W., Krawitz, A.R., Chai, J., Li, W., Zhang, F., Luo, K., and Shi, Y. (2002). Structural mechanism of Smad4 recognition by the nuclear oncoprotein Ski: insights on Ski-mediated repression of TGF- β signaling. *Cell* 111, 357–367.

Xu, L., Wei, Y., Reboul, J., Vaglio, P., Shin, T.H., Vidal, M., Elledge, S.J., and Harper, J.W. (2003). BTB proteins are substrate-specific adaptors in an SCF-like modular ubiquitin ligase containing CUL-3. *Nature* 425, 316–321.

Yeh, W.H. (1991) Genes acting late in the signaling pathway for *Caenorhabditis elegans* dauer larva development. PhD thesis, University of Missouri-Columbia, Columbia, Missouri.

Young, J.C., Obermann, W.M., and Hartl, F.U. (1998). Specific binding of tetratricopeptide repeat proteins to the C-terminal 12-kDa domain of hsp90. *J. Biol. Chem.* 273, 18007–18010.

Note Added in Proof

da Graca et al. have recently reported the identification of DAF-5 as a Ski oncoprotein homolog (*Development* 131, 435–446 [2004]).